A New Experimental Technique for the Measurement of Mass Transfer Rate in Tubular Reactors

CARL M. KOCH

General Electric Company, Philadelphia, Pennsylvania 19101

and

IRAJ ZANDI

Department of Civil and Urban Engineering
University of Pennsylvania, Philadelphia, Pennsylvania 19104

The purpose of this paper is to describe a new experimental technique for studying mass transfer rates in gas/liquid flow in horizontal pipelines. The technique is characterized by the novel use of a magnetic device for the propulsion of the air/liquid medium through a closed circular pipeline. This provides a long duration continuous flow regime uninterrupted and uninfluenced by the turbulence associated with closed loop systems employing conventional pumps for propulsion. The technique represents a unique and innovative approach to the measurement of mass transfer properties in tubular reactors.

APPARATUS DESCRIPTION

Figure 1 depicts the key elements of the experimental apparatus. The magnetic driving force is generated by two magnetic components designated as the external and internal assemblies.

The internal magnet is comprised of a cylindrical permanent magnet with ingot iron pole pieces sized to increase the diameter of the core magnet to within 0.64 cm of the inside diameter of the tubing being used for the circular pipeline. The internal magnet is then fitted with flexible washers sized to provide a tight seal when placed inside the tubing. In the apparatus constructed by the authors the circular pipeline was fabricated from a 12.2-m length of 5.1-cm inside diameter translucent polyethylene tubing with a 0.64 cm wall thickness.

The internal magnet is then placed inside the tubing and the tubing is closed upon itself to form a sealed circular loop. A support structure is required to shape the tubing into a smooth circle, to provide rigidity, and to provide a track for the external magnet assembly. (See Figure 1.)

The external magnet assembly is comprised of three horseshoe magnets rated at a contact lifting force of 1550 N mounted to a carriage. (See Figure 1.) The horseshoe magnets are equipped with curved ingot iron pole pieces to minimize the distance between the external magnet and the outside diameter of the tubing. The external magnet carriage is assembled around the polyethylene tubing with one magnet located on the top of the tubing and the remaining two on the opposite sides of the tubing. The poles of the external magnets are aligned in opposite orientation to those of the internal magnet. In this configuration, movement of the external magnet results in movement of the internal magnet in the same direction via the magnetic attractive force. Movement of the external magnet at any desired velocity is accomplished through a boom connecting the external magnet carriage to a drive motor located at the geometric center of the tubing loop. (See Figure 1.)

The magnetic drive apparatus described above is supplemented with a secondary sampling system connected to the tubing to fulfill the following functions: (1) to provide a facility for injecting fluid, air, and chemicals into the system; (2) to provide for the installation and maintenance of the required sensors; and (3) to provide a mechanism for bleeding air and removing batch samples from the circular pipeline. Figure 2 shows the sampling loop and the instrumentation. More information concerning instrumentation and their calibrations can be found elsewhere (Koch, 1972).

OPERATION OF THE APPARATUS

The following description briefly summarizes the procedure used by the authors in operating the apparatus for the measurement of mass transfer rates.

At the onset of each experiment the circular loop is filled with the fluid under study and all air is bled from the loop. A solution of sodium sulfite is used to reduce the dissolved oxygen (DO) concentration to a desired level and is introduced through the secondary sampling loop. The speed of the finger pump is carefully adjusted during

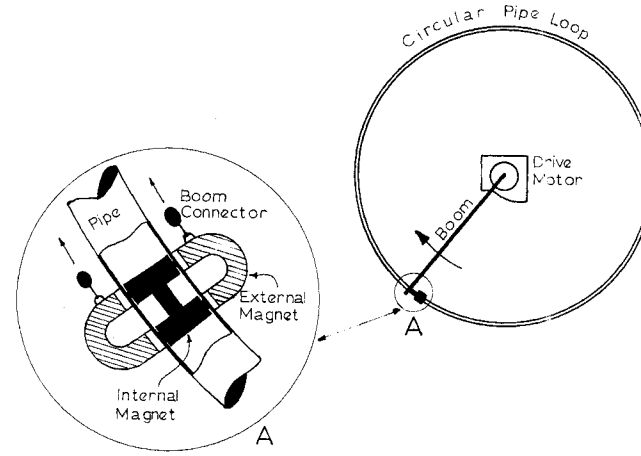

Fig. 1. Diagram of experimental apparatus.

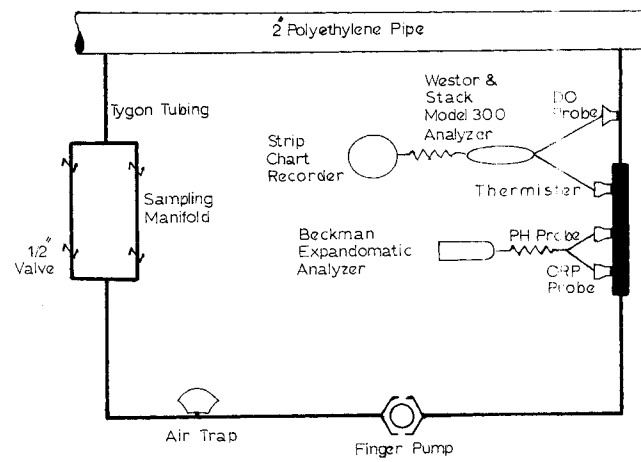

Fig. 2. Schematic of sampling loop.

the sulfite injection so that the sulfite solution is uniformly injected during one complete revolution of the magnetic carriage. A typical oxygen depletion curve is of an exponential shape such as the one shown in Figure 3. The external magnetic carriage is rotated at a fixed speed to obtain the desired liquid velocity. After the dissolved oxygen has stabilized at a new level following sulfite injection, air, or oxygen can be introduced in measured volumes through the secondary sampling loops. Figure 4 indicates a typical oxygen recovery curve obtained by the authors.

The oxygen recovery curves were analyzed by the authors in the conventional manner utilizing Equation (1),

$$\frac{dC}{dt} = K_L A(C^* - C) \qquad (1)$$

where t = time, $K_L A$ = volumetric mass transfer coefficient, C = dissolved oxygen concentration at time t, and C^* = saturation dissolved oxygen concentration. The value of the volumetric mass transfer coefficient $K_L A$ was determined by the differential method. In this method the dissolved oxygen concentration C is plotted against the slope of the oxygen recovery curve dC/dt for different points in time. The slope of a straight line fitted to the data yields the inverse of the volumetric mass transfer coefficient $K_L A$. Alternate methods for analyzing oxygen recovery curves to determine the mass transfer coefficient can also be utilized (Bandyopadhyay, 1969). Values of $K_L A$ can be determined for different liquid velocities by varying the speed of the magnetic plunger.

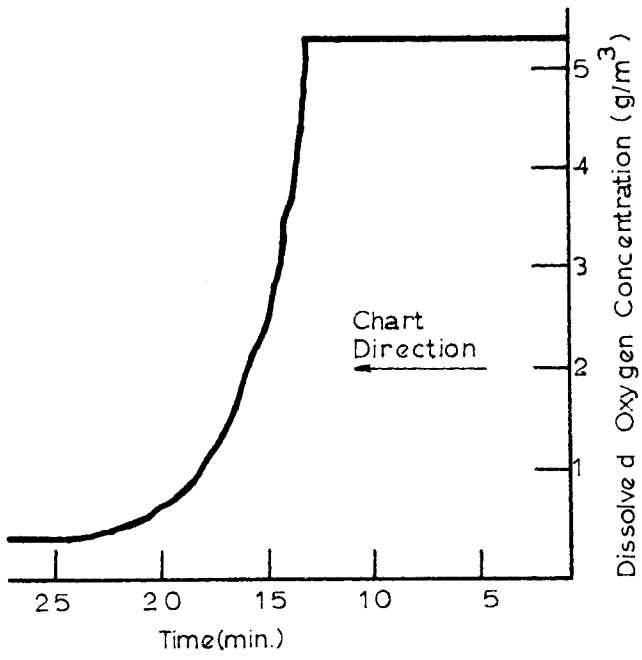

Fig. 3. Typical dissolved oxygen depletion curve.

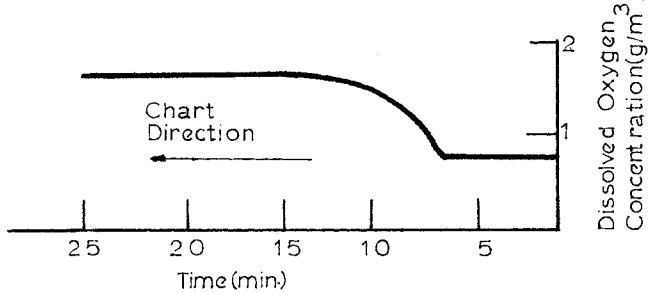

Fig. 4. Typical dissolved oxygen recovery curve.

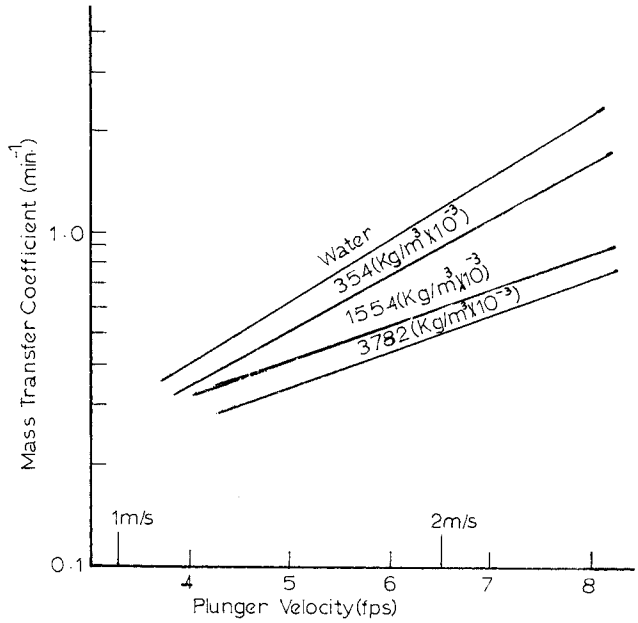

Fig. 5. Curves fitted to the mass transfer coefficient data as a function of slurry velocity and concentration.

The regime of flow can be observed by backlighting the translusive pipe and photographing the flow with a movie camera. The authors observed that the flow regimes established within the range of their experiments were stable for long durations of time. Bubble patterns persisted with little apparent slip or gas accumulation at the plunger interface. Within the range of experiments performed by the authors, (plunger velocities of 0.9 m/s to 2.4 m/s and volumetric air to liquid ratios of 0.01 to 0.04) the regime of flow visually observed appeared to represent bubble flow (Anderson and Russell, 1965).

EXPERIMENTAL RESULTS

The authors employed the apparatus described above to measure order of magnitude mass transfer coefficients for the transfer of oxygen in newspaper slurries. The research was directed at evaluating the feasibility of in-pipeline treatment of sewage-solid waste slurries (Koch and Zandi, 1973).

Newspaper slurries of concentrations of 0.354, 1.554 and 3.782 kg/m^3 (dry weight) were tested to simulate different solid waste slurries. Several slurry velocities were tested within the range of .9 m/s to 2.4 m/s for each concentration. The volumetric mass transfer rates for several air injections were calculated from the oxygen recovery curves and averaged for each velocity range tested. Volumetric gas to liquid ratios were held constant in the range of 0.01 to 0.04.

Figure 5 summarizes a semilogarithmic plot of the mass transfer rates, $K_L A$ values, as a function of the slurry or plunger velocity for water and the three concentrations of newsprint. A detailed discussion of the data and results can be found elsewhere since space does not permit their detailed discussion in this article (Koch, 1972). Suffice it to say that in general $K_L A$ seems to vary directly with slurry velocity and inversely with slurry concentration.

CONCLUSIONS

This paper describes a new experimental technique for studying mass transfer in tubular reactors. While the authors applied the technique to evaluating the mass transfer coefficients for air/solid waste slurries, the technique can be employed for other materials.

LITERATURE CITED

Anderson, R. J., and T. W. F. Russell, "Designing for Two-Phase Flow," *Chem. Eng.* (Dec. 6, 1965).

Bandyopadhyay, B., "Development of a Dynamic Technique for Measuring Volumetric Oxygen Transfer Rates in Aerobic Fermentations—Its Utility and Limitations," Ph.D. dissertation, Univ. Pennsylvania, Philadelphia (1969).

Koch, C. M., "Design and Operation of an Experimental Facility for the Measurement of Mass Transfer Properties in Pipeline Reactors," Ph.D. dissertation, Univ. Pennsylvania, Philadelphia (1972).

———., and I. Zandi, "Use of Pipeline as Aerobic Biological Reactor for Waste Treatment," *J. Water Pollu. Control Fed.*, in press.

Manuscript received October 3, 1972; revision received August 10 and accepted August 13, 1973.

On the Crystal Size Intensity Function and Interpreting Population Density Data from Crystallizers

Y. A. LIU

Department of Chemical Engineering
Princeton University
Princeton, New Jersey 08540

In recent literature the application of the ideal mixed suspension, mixed product removal (MSMPR) crystallizer concept to the analysis of crystal size distribution (CSD) data obtained from experimental or plant crystallizers has been considered. Several excellent reviews are available. Notable have been the works of Randolph (1965), Randolph and Larson (1971), Canning (1970), Nyvlt (1969, 1971), and Mullin (1972). Examination of previous work shows that there still exist many unsolved problems between the various model-oriented interpretations and the actual population density CSD data. There has been criticism of these interpretations from industrial workers as "giving little insight to the actual mechanism" to the real crystallization process involved (Canning, 1970). In addition, many possible combinations of these specific interpretations, such as size-dependent growth rate (Abegg et al., 1968; Bransom, 1960; Canning and Randolph, 1967; and Margolis et al., 1971), size-dependent supersaturation (Estrin, et al., 1969), size-dependent residence time (Randolph and Larson, 1971), and crystal breakage (Rosen and Hulburt, 1971) can apparently fit the same population density CSD data. A typical example is the case of CSD data showing linear sections of different slopes in a semi-log population density distribution plot, $\ln n(L)$ versus L.

In this note, several different interpretations of population density CSD data from crystallizers are re-examined. The crystal size intensity function (CSIF) concept as suggested by the analogous residence time intensity function of Noar and Shinnar (1963) is introduced. It is suggested that this CSIF can be conveniently used together with the population density distribution function developed by Randolph and Larson (1962) in the analysis of CSD data. It makes a distinction among different possible mechanisms leading to similar CSD plots and gives better understanding of implications of previous publications. Certain new insights to clarify the apparent anomalies existing in previous interpretations are also discussed.

CRYSTAL SIZE INTENSITY FUNCTION

It has been shown that steady state crystal size distributions from a continuous MSMPR crystallizer for a number of systems satisfy the solution of the population balance equation (Randolph and Larson, 1962)

$$n = \frac{(rn)^0}{r} \exp\left[- \int_0^L \frac{dL}{rT} \right] \tag{1}$$

For the case of size-independent growth rate, (1) becomes

$$n = n^0 \exp[- L/rT] \tag{2}$$

The simplifying assumptions incorporated in the development of these expressions are well known (Randolph and Larson, 1962 and 1971). The physical meaning of $n(L)$ is as follows: $n(L)dL$ represents the total number of crystal particles of all possible sizes in a unit volume of slurry in the crystallizer that will leave the unit volume of slurry within a particle size between L and $(L + dL)$. If, alternatively, $n(L)$ is considered as a properly normalized probability density distribution function, then, on viewing crystal particles with all possible sizes which have just entered the unit volume of slurry with a particle size between L and $(L + dL)$ is equal to $n(L)dL$. Thus, the population density distribution function $n(L)$ characterizes the CSD for all possible particle sizes.

Consider now a situation where knowledge about the CSD and its related probability information for crystal particles of a specific size is desired. For example, when a selective fines trap is added to a continuous MSMPR crystallizer (Nauman, 1971), knowledge about crystal particles with the specific fines destruction size is particularly important. In this case, a more general problem may be posed: suppose crystal particles with a specific size L have already stayed in a unit volume of slurry in the crystallizer, one desires to know the probability of their leaving the unit volume of slurry within the next size increment dL after growth. Let this conditional prob-